Considerations for DD Simulation at Cryogenic Temperature

Seonghoon Jin, Anh-Tuan Pham, Woosung Choi
Device Lab, AHQ(DS) R&D
Samsung Semiconductor Inc.
San Jose, CA, USA
Email: s.jin@samsung.com

Mohammad Ali Pourghaderi, Uihui Kwon, Dae Sin Kim
CSE Team, Data & Information Technology Center
Samsung Electronics
Hwasung-si, Gyeonggi-do, Korea

***Abstract*—We discuss device models employed in the drift-diffusion simulation of MOSFET transistors at deep cryogenic temperatures. We report potential issues of the commonly used models (the Philips unified mobility model, the high field saturation model, the incomplete ionization model, and the quantization model) at low temperatures and how to resolve the issues. In addition, we present a band tail model to capture the subthreshold slope saturation at low temperatures. We also discuss how to obtain the initial solution and perform the bias ramping to avoid convergence issues. As an application, we study the temperature-dependent operation of a gate-all-around transistor down to 4 K.**

I. Introduction

MOSFET Operations at deep cryogenic temperatures have recently gained attention with the advancement of quantum computers [1]. While there exist studies on the drift-diffusion (DD) model at around 77 K [2], [3], DD simulation down to the liquid He temperature ($\simeq$ 4 K) important for quantum applications has not been extensively studied [4]–[7].

TCAD simulation of MOSFET operations at 4 K is quite challenging due to numerical instabilities and model uncertainties. For example, the intrinsic carrier density in Si cannot be represented in double precision at 4 K. With $kT = 0.34$ meV, small fluctuations in electrostatic potential can result in large fluctuations in carrier density. In addition, commonly employed TCAD models can give unexpected results at low temperatures as they are usually developed for the typical operating temperature range ($-55\ ^\circ\mathrm{C} < T < 150\ ^\circ\mathrm{C}$).

This paper presents a few practical considerations which are relevant to enable DD simulations at deep-cryogenic temperatures. As an application, we study the temperature-dependent operation of a gate-all-around transistor (GAAFET) down to 4 K using our in-house device simulator.

II. Models for Bulk Properties

A. Philips Unified Mobility Model

The first model to consider is the Philips unified mobility model [8], [9]. While it is the standard model to consider bulk mobility, it can cause instabilities at very low temperatures due to the $G(P)$ function which represents the ratio of the majority to minority carrier mobility as shown in Fig. 1. When $T \leq 55$ K (70 K) for electrons (holes), $G(P)$ can have negative values, which results in unphysical mobility values. To fix this issue, the following simple correction to the $G(P)$ function:

$$G \leftarrow 10^{-2} \exp\left[\left(G - 10^{-2}\right)/10^{-2}\right] \quad \text{when } G < 10^{-2} \quad (1)$$

is introduced to prevent $G(P)$ from becoming negative at low temperatures. In addition, the temperature exponent of the lattice scattering mobility term is slightly updated to capture the temperature dependence at low temperature, as shown in Fig. 2.

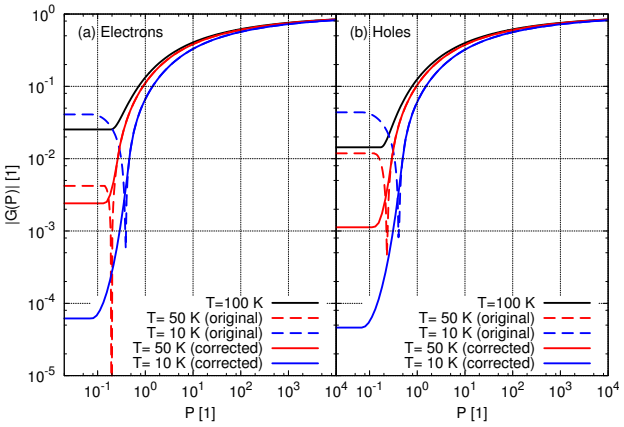

Fig. 1. The ratio of the majority to minority carrier mobility, G, as a function of the parameter P in the Philips unified mobility model [8], [9]. The $G(P)$ can have negative values when $T \leq 55$ K (70 K) for electrons (holes), which results in unphysical mobility values. A simple correction to the $G(P)$ function ($G \leftarrow 10^{-2} \exp\left[\left(G - 10^{-2}\right)/10^{-2}\right]$ when $G < 10^{-2}$) is introduced to prevent $G(P)$ from becoming negative at low temperatures.

B. High Field Saturation Model

The second model to consider is the high field saturation model. For room temperature simulations, we typically employ the Canali model [14]. However, the Canali model gives inaccurate results at low temperatures, as shown in Fig. 3 (b) and (d). On the other hand, the Selberherr model [2] can provide much better results at low temperatures (Fig. 3 (a) and (c)). For electron mobility, we employed the original parameter set from [2]. For hole mobility, we slightly adjusted the saturation velocity $v_{\mathrm{p}}^{\mathrm{sat}}$ and the β parameter as follows:

$$v_{\mathrm{p}}^{\mathrm{sat}} = 9.5 \cdot 10^6\ \mathrm{cm/s} \cdot \sqrt{\tanh\left(\frac{312\ \mathrm{K}}{T}\right)} \quad (2)$$

978-1-6654-0685-7/21/$31.00 ©2021 IEEE

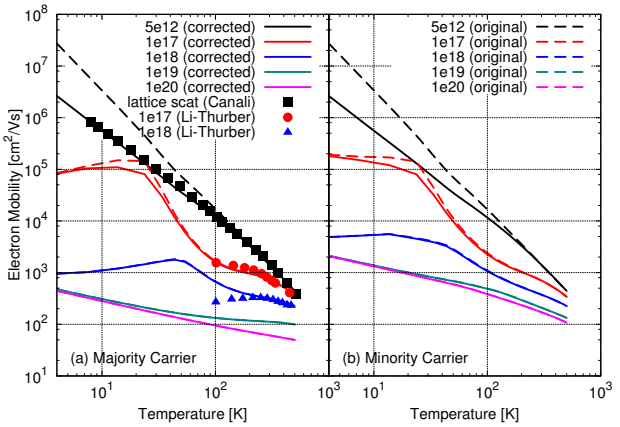

Fig. 2. Temperature dependence of the low-field electron mobility obtained from the Philips unified mobility model [8], [9] for different doping concentrations. Compared with the original model (dashed line), the temperature exponent of the lattice scattering mobility term is changed to $\theta = \theta_0 + \theta_T [\tanh(T/T_0) - 1]$ with $\theta_0 = 2.285$, $\theta_T = 0.55$, and $T_0 = 250$ K. The symbols are from the theoretical and experimental data from [10], [11]. Incomplete ionization model from [12], [13] is employed.

$$\beta = 0.823 + 0.39 \cdot \left(\frac{T}{300\ \mathrm{K}} \right)^{0.5} \tag{3}$$

where T is the lattice temperature. The differences with respect to the experiment at very low temperatures may be related to the field-induced impurity ionization [7], [10]. We also don't recommend overfitting this behavior with too small β parameter [14] as it can cause unphysical results as well as convergence issues.

C. Incomplete Ionization Model

The third model is the incomplete ionization model. For TCAD simulations, the conventional model [16] has been traditionally employed with Boltzmann statistics [3]. However, this model cannot give full ionization in the high concentration limit when used with Fermi statistics, as shown in Fig. 4 (b). On the other hand, the Altermatt model [12], [13] gives consistent results for both types of carrier statistics (see Fig. 4). To obtain consistent results with Fermi statistics, we implement the 'full model' based on the quasi-Fermi potential ((5) in [13]) rather than the 'device model' described in the original paper ((8)–(10) in [13]).

III. Models for MOSFET Simulations

A. A Simulation Setup

As an application, we study the temperature-dependent operation of a 3D GAAFET as shown in Fig. 5. The Poisson, electron and hole continuity, and electron density-gradient equations are solved self-consistently by the fully coupled Newton method. The Philips unified [8], [9] and Lombardi [17], [18] mobility models are employed for the low-field mobility calculations together with the high-field velocity saturation model [2]. The Altermatt incomplete ionization model [12], [13] is considered both for the space charge and the mobility.

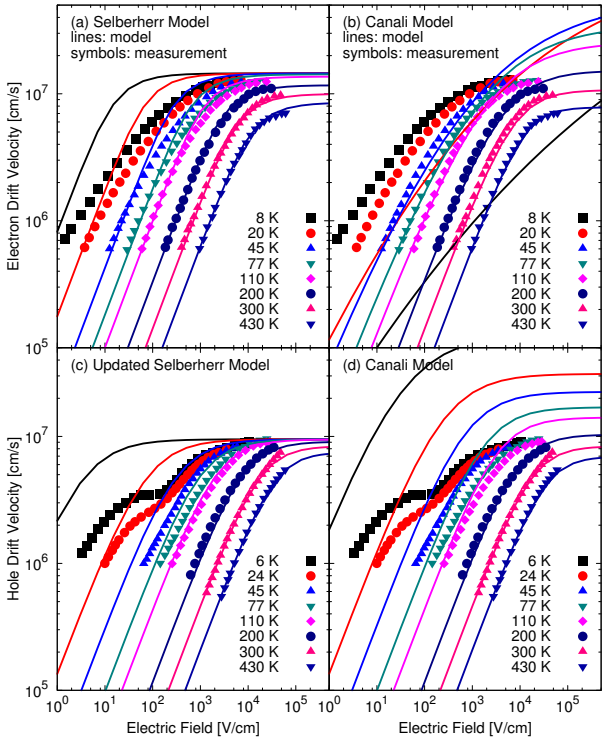

Fig. 3. Comparison of the carrier velocity-field relation for different temperatures obtained from the Selberherr model [2] [(a) and (c)] and the Canali model [14] [(b) and (d)] with the measurement data [10], [15]. The Selberherr model is suitable for DD simulations at low temperatures. For (a), the original parameter set from [2] is employed. For (c), the saturation velocity v_p^{sat} and the β parameter are given by (2) and (3), which is slightly different from [2].

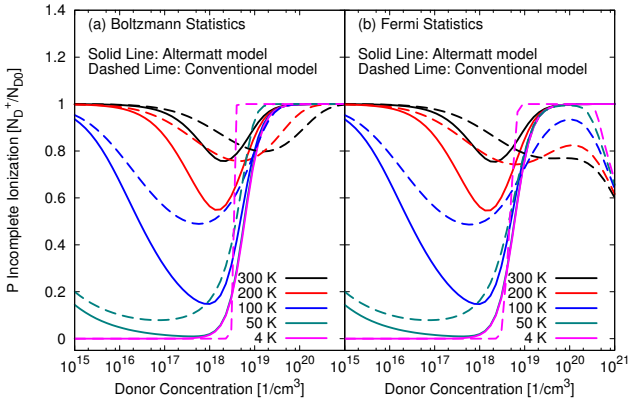

Fig. 4. Comparison of the incomplete ionization models (conventional model [16] (dashed lines) and Altermatt model [12], [13] (solid lines)) with (a) Boltzmann Statistics and (b) Fermi statistics. For both Boltzmann and Fermi statistics, the Altermatt model provides the expected full ionization due to the Mott (metal-insulator) transition in the high concentration limit.

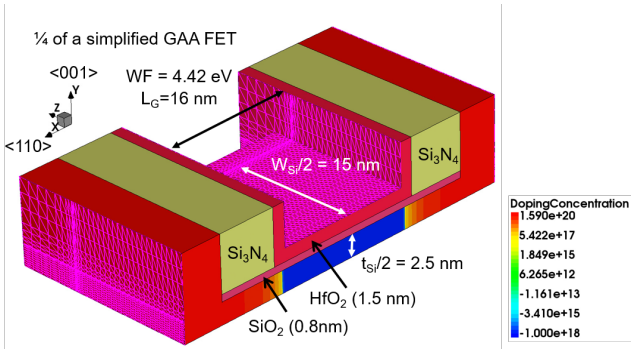

Fig. 5. Simulated 1/4 of 3D GAAFET structure. The Poisson, the electron and hole continuity, and the electron density-gradient equations are solved self-consistently by the fully coupled Newton method. Fermi statistics is used. Philips unified [8], [9] and Lombardi [17], [18] mobility models are employed for the low-field mobility together with the high-field velocity saturation model from [2]. Incomplete ionization model from [12], [13] is considered both for the space charge and the mobility (neutral impurity scattering is neglected). The quantum correction along the transport direction is turned off.

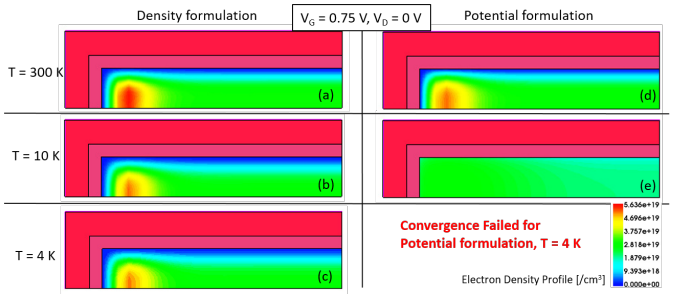

Fig. 6. Comparison of the electron density profile at the center of the GAAFET obtained from the density-gradient model with the original density formulation [19] ((a), (b), and (c)) and the potential-based formulation [20] ((d) and (e)). Only the density-based formulation gives a proper confinement behavior near the Si/SiO_2 interface at low temperatures. In addition, potential-based formulation causes convergence issues at 4 K.

B. Density-Gradient Model

As for the density-gradient model, there exist two different formulations: the original model based on the carrier density [19] and the quantum potential-based model [20]. When Boltzmann statistics is employed, the two models give essentially the same results. With Fermi statistics, however, they can give significantly different results at low temperatures due to the degeneracy effects (see Fig. 6). Only the density-based formulation provides proper quantization at low temperatures. In addition, the unphysical behavior of the potential-based model can also cause convergence issues below 10 K.

C. Initial Solution and Bias Ramping

At low temperatures, obtaining the initial solution of the coupled Poisson and density-gradient equations can be difficult. To get the solution, we multiply a prefactor f to the quantum potential Λ_{n} as

$$\Lambda_{\mathrm{n}} = -f\frac{\hbar^2\gamma}{6m_{\mathrm{n}}}\frac{\nabla^2\sqrt{n}}{\sqrt{n}}, \tag{4}$$

and ramp up f from 0 to 1 to gradually acquire the quantum solution from the classical one (where γ, m_{n}, and n are the quantum potential factor, effective mass, and electron density, respectively).

The bias ramping direction is also important to ensure convergence [6]. For example, we ramp the bias in the following order to obtain the $I_{\mathrm{D}} - V_{\mathrm{G}}$ characteristics for $V_{\mathrm{D}} = 0.75$ V: ($V_{\mathrm{G}} = 0.75$ V, $V_{\mathrm{D}} = 0$ V) $\rightarrow$ (0.75 V, 0.75 V) $\rightarrow$ (0 V, 0.75 V). During the gate bias ramping from the on-state to the off-state, we exit the ramping if the drain current becomes smaller than a certain threshold (10^{-15} A).

D. Band Tail Model

Fig. 7 shows the calculated $I_{\mathrm{D}} - V_{\mathrm{G}}$ characteristics for different temperatures. Similar to the experimental results [1], the temperature reduction increases the on-current and the threshold voltage while reducing the subthreshold slope (SS). The DD model predicts that the SS is proportional to the lattice temperature. On the contrary, the experimental SS cannot decrease further once it reaches its lower limit at around 50 K due to the presence of band tails [21], [22]. To capture this effect, we model the electron density due to the band tail as:

$$n_{\mathrm{tail}} = T_0\left(N_{\mathrm{C}}/T\right)/\left\{1+\exp\left[\left(E_{\mathrm{C}}-E_{\mathrm{Fn}}\right)/kT_{\mathrm{x}}\right]\right\} \tag{5}$$

where $T_{\mathrm{x}} = \left(T^8+T_0^8\right)^{1/8}$, N_{c} is the conduction band effective density-of-states, E_{Fn} is the electron quasi-Fermi energy, E_{C} is the conduction band energy (including quantum correction), k is the Boltzmann constant, T is the lattice temperature, and $T_0 = 50K$ is a model parameter. This expression can be regarded as an approximation to the more rigorous formula derived from the exponential band tail [21], [22]. Fig. 8 compares the calculated subthreshold slope as a function of temperature with and without the band tail model. When n_{tail} is added to the electron density, the temperature dependence of the calculated SS becomes similar to the experiment without affecting the on-current.

IV. Conclusion

We have demonstrated that the 3D TCAD simulation of MOSFET operations at temperatures down to 4 K is possible using our in-house device simulator. We have discussed a few considerations for the mobility models, the incomplete ionization model, the quantum correction model, and the band tail model to realize the DD simulation at 4 K.

References

[1] A. Beckers, F. Jazaeri, and C. Enz, "Cryogenic mosfet threshold voltage model," in *ESSDERC 2019-49th European Solid-State Device Research Conference (ESSDERC)*. IEEE, 2019, pp. 94–97.

[2] S. Selberherr, "Mos device modeling at 77 k," *IEEE Transactions on Electron Devices*, vol. 36, no. 8, pp. 1464–1474, 1989.

[3] A. Akturk, J. Allnutt, Z. Dilli, N. Goldsman, and M. Peckerar, "Device modeling at cryogenic temperatures: Effects of incomplete ionization," *IEEE transactions on electron devices*, vol. 54, no. 11, pp. 2984–2990, 2007.

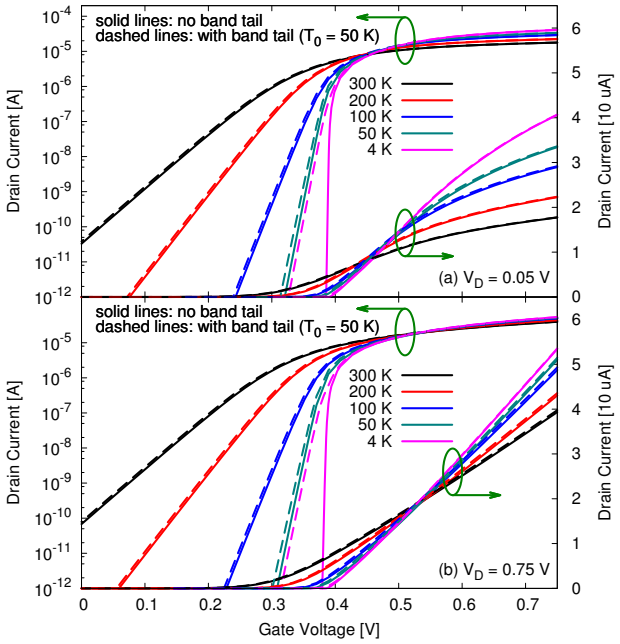

Fig. 7. Calculated $I_{\mathrm{D}} - V_{\mathrm{G}}$ characteristics without the band tail model (solid lines) and with the band tail model (dashed lines). As the temperature is reduced, the subthreshold slope (SS) and the on-current are improved while the threshold voltage is increased.

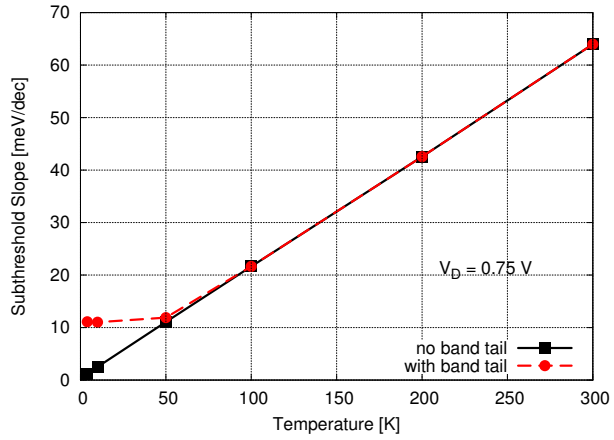

Fig. 8. Calculated subthreshold slope as a function of temperature without the band tail model (black squares) and with the band tail model (red circles). Without the band tail model, the SS is proportional to the lattice temperature. On the other hand, the SS reaches its minimum at around 50 K when the proposed band tail model is employed, which is close to the experimental results [21], [22]. The influence of the band tail is minor when $T > T_0$.

[4] A. Akturk, M. Peckerar, M. Dornajafi, N. Goldsman, K. Eng, T. Gurrieri, and M. Carroll, "Impact ionization and freeze-out model for simulation of low gate bias kink effect in soi-mosfets operating at liquid he temperature," in *2009 International Conference on Simulation of Semiconductor Processes and Devices*. IEEE, 2009, pp. 1–4.

[5] F. A. Mohiyaddin, F. G. Curtis, M. N. Ericson, and T. S. Humble, "Simulation of silicon nanodevices at cryogenic temperatures for quantum computing," *Nanotechnology*, vol. 27, p. 42, 2016.

[6] M. Kantner and T. Koprucki, "Numerical simulation of carrier transport in semiconductor devices at cryogenic temperatures," *Optical and Quantum Electronics*, vol. 48, no. 12, pp. 1–7, 2016.

[7] H. Y. Wong, "Calibrated si mobility and incomplete ionization models with field dependent ionization energy for cryogenic simulations," in *2020 International Conference on Simulation of Semiconductor Processes and Devices (SISPAD)*. IEEE, pp. 193–196.

[8] D. Klaassen, "A unified mobility model for device simulation-I. Model equations and concentration dependence," *Solid-State Electronics*, vol. 35, no. 7, pp. 953–959, 1992.

[9] ——, "A unified mobility model for device simulationII. Temperature dependence of carrier mobility and lifetime," *Solid-State Electronics*, vol. 35, no. 7, pp. 961–967, 1992.

[10] C. Canali, C. Jacoboni, F. Nava, G. Ottaviani, and A. Alberigi-Quaranta, "Electron drift velocity in silicon," *Physical Review B*, vol. 12, no. 6, p. 2265, 1975.

[11] S. S. Li and W. R. Thurber, "The dopant density and temperature dependence of electron mobility and resistivity in n-type silicon," *Solid-State Electronics*, vol. 20, no. 7, pp. 609–616, 1977.

[12] P. Altermatt, A. Schenk, and G. Heiser, "A simulation model for the density of states and for incomplete ionization in crystalline silicon. i. establishing the model in si: P," *Journal of Applied Physics*, vol. 100, no. 11, p. 113714, 2006.

[13] P. Altermatt, A. Schenk, B. Schmithüsen, and G. Heiser, "A simulation model for the density of states and for incomplete ionization in crystalline silicon. ii. investigation of si: As and si: B and usage in device simulation," *Journal of Applied Physics*, vol. 100, no. 11, p. 113715, 2006.

[14] C. Canali, G. Majni, R. Minder, and G. Ottaviani, "Electron and hole drift velocity measurements in silicon and their empirical relation to electric field and temperature," *IEEE Trans. Electron Devices*, vol. 22, no. 11, pp. 1045–1047, 1975.

[15] C. Jacoboni, C. Canali, G. Ottaviani, and A. A. Quaranta, "A review of some charge transport properties of silicon," *Solid-State Electronics*, vol. 20, no. 2, pp. 77–89, 1977.

[16] M. R. Shaheed and C. M. Maziar, "A physically based model for carrier freeze-out in Si- and SiGe-base bipolar transistors suitable for implementation in device simulators," in *Bipolar/BiCMOS Circuits & Technology Meeting*, 1994, p. 191.

[17] C. Lombardi, S. Manzini, A. Saporito, and M. Vanzi, "A physically based mobility model for numerical simulation of nonplanar devices," *IEEE Trans. Comput.-Aided Design Integr. Circuits Syst.*, vol. 7, no. 11, p. 1164, Nov. 1988.

[18] M. Darwish, J. Lentz, M. Pinto, P. Zeitzoff, T. Krutsick, and H. Vuong, "An improved electron and hole mobility model for general purpose device simulation," *IEEE Trans. Electron Devices*, vol. 44, no. 9, p. 1529, Sep. 1997.

[19] M. Ancona and G. Iafrate, "Quantum correction to the equation of state of an electron gas in a semiconductor," *Physical Review B*, vol. 39, no. 13, p. 9536, 1989.

[20] A. Wettstein, A. Schenk, and W. Fichtner, "Quantum device-simulation with the density-gradient model on unstructured grids," *IEEE Trans. Electron Devices*, vol. 48, no. 2, pp. 279–284, 2001.

[21] H. Bohuslavskyi, A. Jansen, S. Barraud, V. Barral, M. Cassé, L. Le Guevel, X. Jehl, L. Hutin, B. Bertrand, G. Billiot *et al.*, "Cryogenic subthreshold swing saturation in fd-soi mosfets described with band broadening," *IEEE Electron Device Letters*, vol. 40, no. 5, pp. 784–787, 2019.

[22] A. Beckers, F. Jazaeri, and C. Enz, "Theoretical limit of low temperature subthreshold swing in field-effect transistors," *IEEE Electron Device Letters*, vol. 41, no. 2, pp. 276–279, 2019.